Supplementary online information for: Crystal Packing and Molecular Conformation of Nitrocellulose from Fiber X-ray Diffraction and Molecular Dynamics Simulations

Edmund Morris[1], Pawel Sikorski[2*], Anna Warren[3], Sofia Jaho[3], Colin R. Pulham[1], Carole A. Morrison[1*]

[1*]School of Chemistry and EaStCHEM Research School, University of Edinburgh, The King's Buildings, David Brewster Road, Edinburgh, EH9 3FJ, UK.
[2]Department of Physics, Norwegian University of Science and Technology, NTNU, Høgskoleringen 5, Trondheim, 7491, Norway.
[3]Diamond Light Source, Harwell Science and Innovation Campus, Didcot, OX11 0DE, UK.

*Corresponding author(s). E-mail(s): pawel.sikorski@ntnu.no; c.morrison@ed.ac.uk;
Contributing authors: edmund.morris@ed.ac.uk; anna.warren@diamond.ac.uk; sofia.jaho@diamond.ac.uk; c.r.pulham@ed.ac.uk;

Supplementary Information for Molecular Dynamics Simulations

Shown in Figure S1 is the heatmap of the two glycosidic torsional angles, ϕ (O-C-O-C) and Ψ (C-O-C-C), obtained from the 5 ns production run MD trajectory (3 x 3 x 1 supercell; 100 evenly spaced frames). The resulting averaged values (ϕ (O-C-O-C) = -79 +/- 25 degrees and Ψ (C-O-C-C) = 112 +/- 4 degrees align well with the minimum energy basin previously reported in MD simulations of polysaccharide chains linked by β (1-4) glycosidic bonds by the CHARMM, GLYCAM and GROMOS force fields.[1]

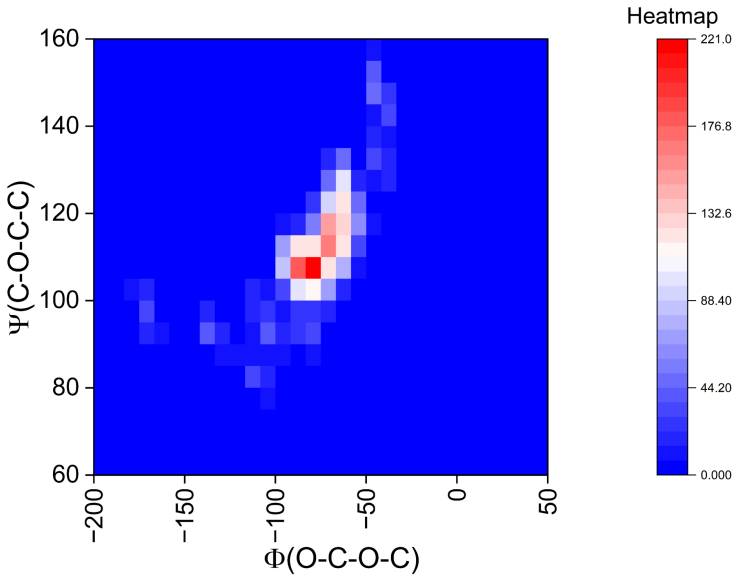

Fig. S1 Heatmap of glycosidic torsional angles derived from the 5 ns MD 3 x 1 x 1 supercell production run trajectory

Figure S2 shows the histogram (presented in 60 degree bins) for the O5-C5-C6-O6 side chain torsions, derived from the time-averaged (single frame) 3 x 3 x 1 supercell model, showing that 25/45 side chains are in the +60 degree (gt) conformation, 15/45 are in the -60 degree (gg) conformation, while 2/45 are in the 180 (tg) orientation.

Figure S3 shows the non-covalent interaction (NCI) plot, generated for the pro-molecular electron density surface, for two neighbouring NC helices, as presented in the 3 x 3 x 1 supercell time-averaged structure. The green discs highlight the significant attractive intermolecular interactions, which are predominantly non-classical C-H...O hydrogen bonds.

Finally, Figure S4 shows the RMSD plot for the 5 ns production run MD trajectory, indicating that a stable simulation model has been obtained.

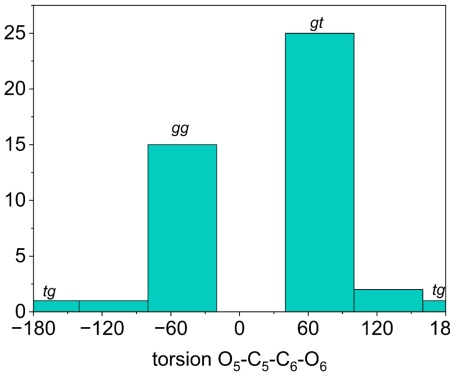

Fig. S2 Histogram of NC side-chain orientations, derived from the time-averaged 3 x 3 x 1 supercell model.

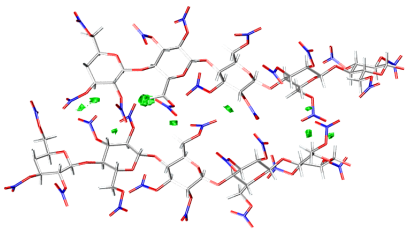

Fig. S3 Non-covalent interaction plot of the promolecular electron density for two neighbouring NC helices present in the 3 x 3 x 1 supercell time-averaged structure.

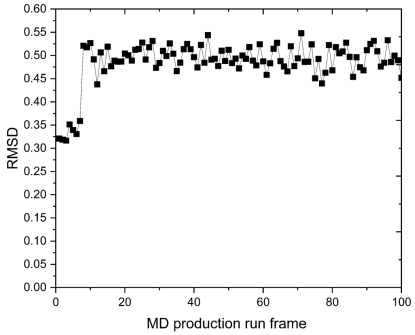

Fig. S4 RMSD plot for the 5 ns production run trajectory, derived for the 3 x 3 x 1 supercell model of NC using the COMPASS force field.

Supplementary Information for Determination of the Unit Cell Parameters

Experimental data impose constraints on the possible values of the unit cell parameters. However, the same set of reflections can be interpreted by a range of unit cell shapes, with interdependent relationships among the parameters governed by the constraints. Figure S5(a) illustrates how the a, b, β, and γ parameters vary as a function of the unit cell angle α. In principle, all combinations shown satisfy the experimental constraints. Nevertheless, the diffraction pattern reveals a signal on the 7th and 10th layer lines (ll) near the meridian, while no signal is observed on the 5th ll. To identify the unit cell that best matches the observed pattern, we plot the spacing of the reflection closest to the meridian on the 5th, 7th (b), 10th (c) and 1st (d) ll.

For $\alpha = 108°$, no lattice point—and thus no reflection—is predicted on the meridian for the 5th ll, consistent with the absence of signal. In contrast, a reflection is predicted on the 7th ll, aligning with the experimental observation. The same holds true for the 10th ll, where a lattice point near the meridian is also predicted. Additionally, this α angle yields the correct spacing for the reflections observed on the 1st ll.

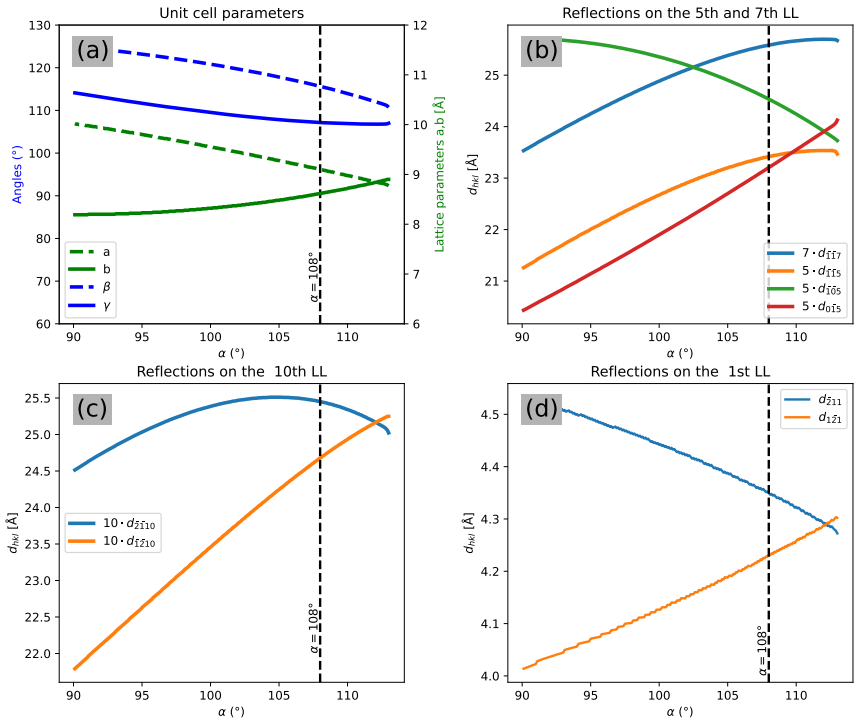

Fig. S5 Unit cell parameters (a) and predicted lattice points close to the meridian for 5th and 7th layer lines (b), 10th layer line (c) and 1st layer line (d).

Supplementary Information for the Processing of Fibre Diffraction Patterns

Data from the I24 and VMXm beamlines were exported as 32-bit Tagged Image File Format (TIFF) files using the DAWN software suite for subsequent processing and analysis of the diffraction patterns. These unprocessed files are available in the ESI.

I24 Tilt series - Figure 1

For the tilt series, a background diffraction pattern of equivalent exposure was collected and subtracted from each frame to account for air scattering and other ambient background signals.

VMXm summed diffraction pattern - Figure 2

The diffraction patterns for the summed image were collected as a grid scan at the VMXm beamline. No background subtraction was applied to these images as they were collected under vacuum. These images were manually screened to select for high signal-to-noise ratio. Each of the selected TIFF files was then individually rotated to orient the high-intensity equatorial signals horizontally. The images were summed pixel-by-pixel using the NumPy library in a custom Python script. The use of the 32-bit TIFF format ensured that the final, summed pixel intensity values remained within the available range of 2^{32} possible values, preventing data saturation or clipping.

References

[1] Lutsyk, V., Wolski, P., Plazinski, W.: The Conformation of Glycosidic Linkages According to Various Force Fields: Monte Carlo Modeling of Polysaccharides Based on Extrapolation of Short-Chain Properties. Journal of Chemical Theory and Computation **20**(14), 6350–6368 (2024) https://doi.org/10.1021/acs.jctc.4c00543 . Publisher: American Chemical Society